

Note

Synthesis and structure of the monometallic cationic complex [Cp(CO)₂Fe{η²-(CH₂CHCH₂CH₃)}]PF₆ (Cp = η⁵-C₅H₅)

Evans O. Changamu^a, Holger B. Friedrich^{a,*}, Melanie Rademeyer^b

^a School of Chemistry, University of KwaZulu-Natal, Durban 4041, South Africa

^b School of Chemistry, University of KwaZulu-Natal, Private Bag X01, Scottsville, Pietermaritzburg 3209, South Africa

Received 24 August 2007; received in revised form 4 October 2007; accepted 8 October 2007

Available online 14 October 2007

Abstract

The bimetallic carbocation complex [(Cp(CO)₂Fe)₂(μ-C₄H₇)]PF₆ reacted with trifluoroacetic acid to give the mononuclear cationic complex [Cp(CO)₂Fe{η²-(CH₂CHCH₂CH₃)}]PF₆, which formed yellow orthorhombic crystals in the space group *P*2₁2₁2₁ with *a* = 7.652(4), *b* = 13.422(7), *c* = 14.037(7); α = β = γ = 90.00 and *Z* = 4. The carbocation is coordinated to the metal in a η²-fashion forming a chiral metallacyclopropane type structure. The β-CH carbon (C9) is disordered over two positions (C9A and C9B), each having about 50% occupancy. This is attributed to there being both the *R* and *S* enantioface isomers in equal amounts in the crystal sample. NMR data indicate that the metallacyclopropane structure observed in the solid state is preserved in solution.
© 2007 Elsevier B.V. All rights reserved.

Keywords: Metallacyclopropane; Mononuclear carbocation complex; Iron

1. Introduction

Mononuclear iron carbocation complexes of the types [Cp(CO)₂Fe(CH₂CHR)]X (X = anion such as PF₆⁻, BF₄⁻, R = H, alkyl or aryl group) have been fairly extensively studied [1–7], but none have been structurally characterized. The only related complexes that have been structurally characterized include [Cp(CO)₂Fe(CH₂CHNMe₂)]PF₆ [7,8], [Cp(CO)₂Fe(CH₂CHOMe)]PF₆ [7] and [Cp(CO)₂Fe(CH₂CHOEt)]PF₆ [8], where the alkyl group includes a heteroatom. The rhenium analogues including the 3-methylbut-1-ene complex (*RS,SR*)-[CpRe(NO)(PPh₃){CH₂=CHCH(CH₃)₂}]BF₄, [9], the styrene complex (*RS,SR*)-[CpRe(NO)(PPh₃)(CH₂=CHC₆H₅)]BF₄ and its corresponding (*RR,SS*) isomer [10], the allylbenzene complex (*RS,SR*)-[CpRe(NO)(PPh₃)(CH₂=CHCH₂C₆H₅)]PF₆ [11], the cyclopentene complex [CpRe(NO)(PPh₃)(cyclopentene)]BF₄ [12] and the *cis*- and *trans*-2-butene complexes (*RSR,SR*) [CpRe(NO)(PPh₃)(CH₃CH=CH-

CH₃)]BF₄ and (*RSS,SRR*)-[CpRe(NO)(PPh₃)(CH₃CH=CHCH₃)]BF₄ [13], respectively, have been reported.

Bonding between alkyl or alkanediyl carbocations and transition metals is believed to be similar to that of coordinated olefins and hence they are considered to be activated olefins. Coordinated olefins are very reactive towards nucleophilic attack [14] and it had been suggested that the activation arises from displacement of the metal fragment, in the course of reaction, toward one end of the olefin (also called “slippage” of the olefin) [15]. Thus, structural determinations of olefin complexes have been undertaken in order to ascertain the presence of olefin “slippage”. In a few of the reported cases the olefin “slippage” has been observed [9,13] while in others very insignificant “slippage” has been reported [11–13]. This partly explains why carbocation complexes are of interest [16].

We recently reported the synthesis and NMR studies of transition metal stabilized mono- and dicarbocationic complexes in which the results clearly showed that the metals form metallacyclopropanes with the carbocationic ligands [17,18]. We now report on the structural

* Corresponding author. Tel.: +27 31 2603107; fax: +27 31 2603091.
E-mail address: friedric@ukzn.ac.za (H.B. Friedrich).

characterization of the mononuclear cationic complex, $[\text{Cp}(\text{CO})_2\text{Fe}\{\eta^2\text{-(CH}_2\text{CHCH}_2\text{CH}_3)\}]\text{PF}_6$ obtained from the bimetallic complex $[\{\text{Cp}(\text{CO})_2\text{Fe}\}_2\{\eta^2\text{-(C}_4\text{H}_7)\}]\text{PF}_6$ by electrophilic substitution. The synthesis of $[\text{Cp}(\text{CO})_2\text{Fe}\{\eta^2\text{-(CH}_2\text{CHCH}_2\text{CH}_3)\}]\text{PF}_6$ by different routes, including hydride abstraction [1] and reduction of 1,2-epoxybutane with $[\text{Cp}(\text{CO})_2\text{Fe}]^-$ [19], has been described previously, but no crystal data were reported. The preparation of the BF_4^- salt by the reaction of σ -allyl complex $[\text{Cp}(\text{CO})_2\text{FeCH}_2\text{CH}=\text{CH}_2]$ with $\text{Me}_3\text{O}^+\text{BF}_4^-$ has also been described [20].

2. Results and discussion

The reaction of the carbocation complex $[\{\text{Cp}(\text{CO})_2\text{Fe}\}_2(\mu\text{-C}_4\text{H}_7)]\text{PF}_6$ with trifluoroacetic acid in THF gave the monometallic cationic complex $[\text{Cp}(\text{CO})_2\text{Fe}\{\eta^2\text{-(CH}_2\text{CHCH}_2\text{CH}_3)\}]\text{PF}_6$ in 95% yield. It was precipitated as a golden yellow solid by the addition of diethyl ether (Scheme 1). It was characterized by elemental analysis, IR and NMR spectroscopy, melting point and X-ray crystallography. The by-product $[\text{Cp}(\text{CO})_2\text{Fe}]_2$ was also isolated. The solid state IR spectrum (KBr) shows two strong C–O stretching bands at 2081 and 2045 cm^{-1} as is expected for cationic complexes of this kind [1,17]. The solution IR spectrum shows two strong C–O stretching

bands at 2075 and 2038 cm^{-1} , positions very similar to those observed in the solid state, indicating that the solid state structure is preserved in solution. No C=C stretching

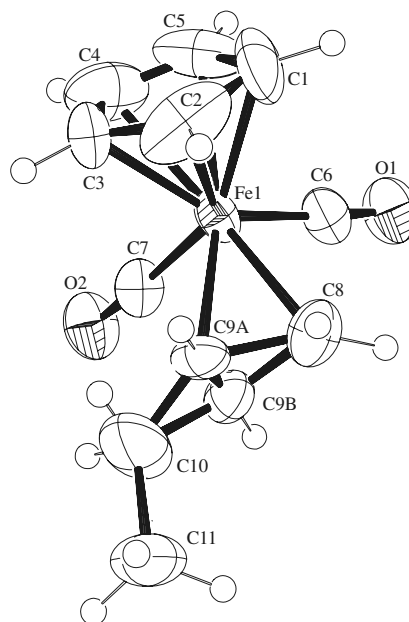
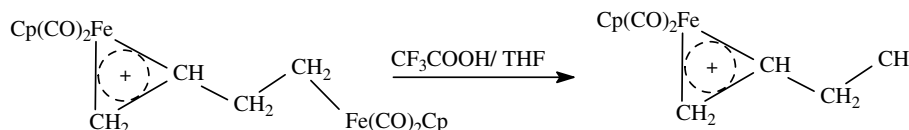


Fig. 2. The ORTEP drawing of the molecular structure of $[\text{Cp}(\text{CO})_2\text{Fe}\{\eta^2\text{-(CH}_2\text{CHCH}_2\text{CH}_3)\}]^+$ showing the numbering scheme of the atoms. Thermal ellipsoids are drawn at 50% probability level.



Scheme 1.

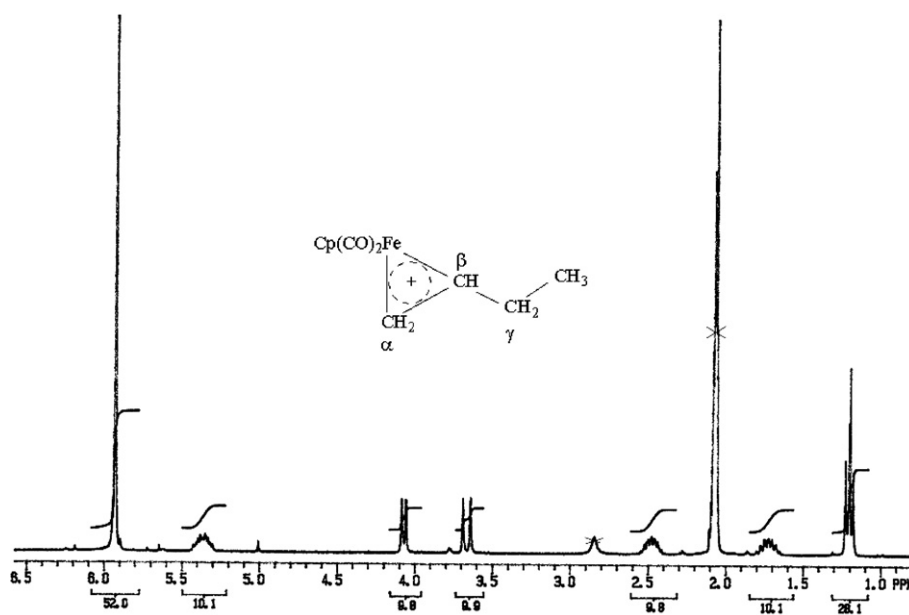


Fig. 1. ^1H NMR spectrum of $[\text{Cp}(\text{CO})_2\text{Fe}\{\eta^2\text{-(CH}_2\text{CHCH}_2\text{CH}_3)\}]\text{PF}_6$ (acetone- d_6) showing the diastereotopic CH_2 protons. Inset: structure of the molecule.

band is seen in the IR spectrum, further supporting the ligand coordination mode shown in Scheme 1.

2.1. ^1H and ^{13}C NMR spectroscopy

Fig. 1 shows the ^1H NMR spectrum of $[\text{Cp}(\text{CO})_2\text{Fe}\{\eta^2\text{-(CH}_2\text{CHCH}_2\text{CH}_3)\}]\text{PF}_6$ recorded at room temperature in acetone- d_6 . The sharpness and pattern of signals in the ^1H NMR spectrum suggest that $[\text{Cp}(\text{CO})_2\text{Fe}\{\eta^2\text{-(C}_4\text{H}_8)\}]\text{PF}_6$ has a rigid chiral structure in solution. The two doublets at 4.05 ppm ($J = 8.2$ Hz) and 3.15 ppm

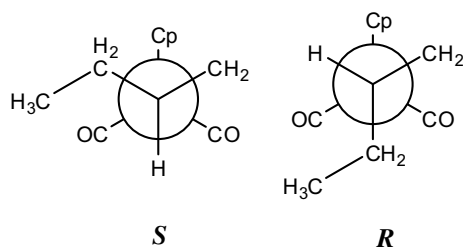


Fig. 3. Idealized structures of the $[\text{Cp}(\text{CO})_2\text{Fe}\{\eta^2\text{-(CH}_2\text{CHCH}_2\text{CH}_3)\}]^+$ cation showing the enantioface binding possibilities of the butyl carbocation.

($J = 14.6$ Hz) were assigned to the diastereotopic $\alpha\text{-CH}_2$ protons which are *cis* and *trans* to the $\beta\text{-CH}^{\delta+}$ proton, respectively, in the molecule. The distinct multiplets at 2.48 ppm and 1.71 ppm were assigned to the diastereotopic $\gamma\text{-CH}_2$ protons. Their nonequivalence is strong evidence that the carbocationic ligand is η^2 -coordinated to the metal [8]. Even rotation about the $\text{C}_\beta\text{-C}_\gamma$ single bond does not result in their equivalence because they are near a chiral centre (the $\beta\text{-CH}^{\delta+}$ carbon). The distinctive triplet due to the CH_3 protons at 1.22 ppm confirms that the presence of the CH_3 group in the ligand $\text{CH}_2\text{CHCH}_2\text{CH}_3$. Heteronuclear Single Quantum Correlation (HSQC) data confirmed that C9 (Fig. 2) is attached to only one proton while C8 and C10 are attached to two diastereotopic protons each.

The ^{13}C NMR spectrum shows the signals due to the α - and β -carbons at 54.5 and 90.4 ppm, respectively. These are significantly shielded relative to the olefinic carbon atoms of 1-butene, suggesting increased electron donation from the metal centre to the formally positive $\beta\text{-CH}$ carbon. The $\gamma\text{-CH}_2$ carbon is also significantly shielded, resonating at about 30 ppm. This would not be expected if the positive charge was localized on the $\beta\text{-CH}$ carbon to which it is directly attached. These observations indicate that the positive charge is delocalized, mainly, within the

Table 1
Selected bond angles and bond lengths for $[\text{Cp}(\text{CO})_2\text{Fe}\{\eta^2\text{-(CH}_2\text{CHCH}_2\text{CH}_3)\}]\text{PF}_6$

Bond lengths (Å)					
C6–Fe1	1.792(3)	C3–Fe1	2.084(4)	C8–C9A	1.389(7)
C1–C5	1.369(7)	C2–Fe1	2.105(4)	C8–C9B	1.419(7)
C1–C2	1.450(6)	C4–C3	1.322(6)	C8–Fe1	2.152(3)
C1–Fe1	2.072(4)	C4–Fe1	2.092(4)	C10–C9B	1.334(8)
C5–C4	1.277(6)	C7–O2	1.119(4)	C10–C9A	1.369(7)
C5–Fe1	2.056(4)	C7–Fe1	1.813(3)	C9A–Fe1	2.301(6)
O1–C6	1.132(3)	C11–C10	1.497(5)	C9B–Fe1	2.173(5)
C2–C3	1.413(6)				
Bond angles (°)					
O1–C6–Fe1	176.4(3)	C10–C9B–C8	134.8(7)	C6–Fe1–C8	83.9(1)
C5–C1–C2	105.5(4)	C10–C9B–Fe1	127.0(5)	C7–Fe1–C8	108.1(1)
C5–C1–Fe1	70.0(3)	C8–C9B–Fe1	70.0(3)	C5–Fe1–C8	140.4(2)
C2–C1–Fe1	70.9(2)	C6–Fe1–C7	92.5(1)	C1–Fe1–C8	102.4(2)
C4–C5–C1	111.9(4)	C6–Fe1–C5	90.2(2)	C3–Fe1–C8	117.2(2)
C4–C5–Fe1	73.6(3)	C7–Fe1–C5	111.3(2)	C4–Fe1–C8	153.1(2)
C1–C5–Fe1	71.3(3)	C6–Fe1–C1	93.7(2)	C2–Fe1–C8	89.6(1)
C3–C2–C1	102.6(3)	C7–Fe1–C1	149.3(2)	C6–Fe1–C9B	117.1(2)
C3–C2–Fe1	69.5(3)	C5–Fe1–C1	38.7(2)	C7–Fe1–C9B	87.4(2)
C1–C2–Fe1	68.5(2)	C6–Fe1–C3	152.0(2)	C5–Fe1–C9B	146.8(3)
C3–C4–C5	109.8(4)	C7–Fe1–C3	97.6(1)	C1–Fe1–C9B	116.0(3)
C3–C4–Fe1	71.2(2)	C5–Fe1–C3	61.8(2)	C3–Fe1–C9B	89.5(3)
C5–C4–Fe1	70.5(3)	C1–Fe1–C3	65.1(2)	C4–Fe1–C9B	124.4(3)
C4–C3–C2	110.2(4)	C6–Fe1–C4	118.3(2)	C2–Fe1–C9B	82.0(3)
C4–C3–Fe1	71.9(3)	C7–Fe1–C4	87.1(2)	C8–Fe1–C9B	38.3(2)
C2–C3–Fe1	71.1(3)	C5–Fe1–C4	36.9(2)	C6–Fe1–C9A	97.0(2)
O2–C7–Fe1	176.6(3)	C1–Fe1–C4	63.6(2)	C7–Fe1–C9A	74.0(2)
C9A–C8–Fe1	77.8(3)	C3–Fe1–C4	36.1(2)	C5–Fe1–C9A	170.9(2)
C9B–C8–Fe1	71.7(3)	C6–Fe1–C2	131.0(2)	C1–Fe1–C9A	134.7(3)
C9B–C10–C11	122.8(5)	C7–Fe1–C2	135.2(2)	C3–Fe1–C9A	110.9(2)
C9A–C10–C11	117.3(4)	C5–Fe1–C2	65.3(2)	C4–Fe1–C9A	140.7(2)
C10–C9A–C8	134.3(7)	C1–Fe1–C2	40.6(2)	C2–Fe1–C9A	105.7(2)
C8–C9A–Fe1	66.1(3)	C3–Fe1–C2	39.4(2)	C8–Fe1–C9A	36.2(2)
C10–C9A–Fe1	116.7(4)	C4–Fe1–C2	64.6(2)		

metallacycle (see Scheme 1). This can also be seen from the significantly deshielded protons of the cyclopentadiene ligand attached to the metal. Similar observations have been made in the NMR spectra of bimetallic carbocation complexes [17,18].

2.2. Crystal structure of $[\text{Cp}(\text{CO})_2\text{-Fe}\{\eta^2\text{-(CH}_2\text{CHCH}_2\text{CH}_3)\}] \text{PF}_6$

The compound formed yellow orthorhombic crystals in the space group $P2_12_12_1$. A suitable crystal was selected and subjected to diffraction studies. The refinement gave the structure shown in Fig. 2 in which atom C9 appears disordered over two positions, with occupancy factors of 0.54 for atom C9A and 0.46 for atom C9B. The metal centre is asymmetrically coordinated to both C8 and C9, with bond lengths of $\text{Fe-C8} = 2.152(3) \text{ \AA}$, $\text{Fe-C9A} = 2.301(6) \text{ \AA}$ and $\text{Fe-C9B} = 2.173(5) \text{ \AA}$.

The observed disorder may be attributed to the presence of two isomers of the compound in the sample crystal. Depending on the enantioface of the butyl carbocation coordinated to the metal, two isomers (i.e. *S* and *R*) are possible for this compound. Fig. 3 shows idealized structures of the possible isomers with the metal (behind the circle) assigned the highest priority and the proton on C9 assigned the lowest priority according to the Cahn–Ingold–Prelog priority rules [21]. After refinement the Flack parameter obtained was 0.49 suggesting that both isomers are present in equal amounts in the crystal sample. Similar disorder was observed in the bimetallic complex $[\text{Cp}^*(\text{CO})_2\text{FeCH}_2\text{CHCH}_2\text{Fe}(\text{CO})_2\text{Cp}^*] \text{PF}_6$ [22].

The bond length Fe-C8 ($\text{Fe-C}\alpha$) = $2.152(3) \text{ \AA}$ is similar to $2.167(5) \text{ \AA}$ and $2.173(2) \text{ \AA}$ reported for the equivalent bond in the bimetallic carbocation complexes $[\text{Cp}^*(\text{CO})_2\text{-Fe}\{\mu\text{-(C}_3\text{H}_5)\}\text{-Fe}(\text{CO})_2\text{Cp}] \text{PF}_6$ [23] and $[\text{Cp}^*(\text{CO})_2\text{-Fe}\{\mu\text{-(C}_3\text{H}_5)\}\text{Ru}(\text{CO})_2\text{Cp}] \text{PF}_6$ [24], respectively. It is also similar to $2.109(10) \text{ \AA}$ reported for the equivalent bond in the complex $[\text{Cp}(\text{CO})_2\text{Fe}(\text{CH}_2\text{CHOCH}_2\text{CH}_3)] \text{PF}_6$ [8]. It is, however, slightly longer than 2.08 \AA reported for the $\text{Fe-C}\alpha$ bond in the neutral complexes $[\{\text{Cp}(\text{CO})_2\text{-Fe}\}_2(\text{CH}_2)_3]$ and $[\{\text{Cp}(\text{CO})_2\text{-Fe}\}_2(\text{CH}_2)_4]$ [25]. The observed $\text{Fe-C}\beta$ bond lengths $\text{Fe-C9A} = 2.301(6) \text{ \AA}$, $\text{Fe-C9B} = 2.173(5) \text{ \AA}$ are close to $2.32(2) \text{ \AA}$ and $2.402(10) \text{ \AA}$ reported for the equivalent bond in the complexes $[\text{Cp}(\text{CO})_2\text{Fe}(\text{CH}_2\text{-CHOCH}_3)] \text{PF}_6$ [16] and $[\text{Cp}(\text{CO})_2\text{Fe}(\text{CH}_2\text{CHOEt})] \text{PF}_6$ [8], respectively. The observed bond lengths $\text{C}\alpha\text{-C}\beta$ ($\text{C8-C9A} = 1.389(7) \text{ \AA}$ and $\text{C8-C9B} = 1.419(7) \text{ \AA}$) are longer than the $1.336(14) \text{ \AA}$ reported for the vinyl ether complex [8], which suggests that there is much more significant single bond character in the $\text{C}\alpha\text{-C}\beta$ bond of the complex $[\text{Cp}(\text{CO})_2\text{Fe}\{\eta^2\text{-(C}_4\text{H}_8)\}] \text{PF}_6$ than in that of the vinyl ether complex $[\text{Cp}(\text{CO})_2\text{Fe}(\text{CH}_2\text{CHOEt})] \text{PF}_6$ [8]. They are, however, within the range of the values observed for the equivalent bonds in the mixed-ligand bimetallic complexes [23,24]. Selected bond lengths and angles are given in Table 1, while crystallographic data collection and analysis details are given in Table 2.

Table 2

Crystal data and structure refinement for $[\text{Cp}(\text{CO})_2\text{Fe}\{\eta^2\text{-(CH}_2\text{CH-CH}_2\text{CH}_3)\}] \text{PF}_6$

Empirical formula	$\text{C}_{11}\text{H}_{13}\text{F}_6\text{FeO}_2\text{P}$
Formula weight (g/mol)	378.03
Lattice	Orthorhombic
Space group	$P2_12_12_1$
Cell dimensions	
a (\AA)	7.652(4)
b (\AA)	13.422(7)
c (\AA)	14.037(7)
α ($^\circ$)	90.00
β ($^\circ$)	90.00
γ ($^\circ$)	90.00
V (\AA^3)	1441.77(13)
Z	4
D_x (Mg m^{-3})	1.783
Temperature (K)	150(2)
Crystal size (mm)	$0.3 \times 0.2 \times 0.2$
$F(000)$	772
μ ($\text{Mo K}\alpha$) (mm^{-1})	1.226
Wavelength (λ)	0.71073 \AA
Reflections for cell parameters	635
Crystal description	Block
Crystal colour	Yellow
Collected data range, 2θ	$3.9294\text{--}32.0450$
Transmission factors (T_{min} : T_{max})	0.7100, 0.7916
Measured reflections	14990
Independent reflections	4657
Observed reflections with $I > 2\sigma(I)$	3006
Internal fit	$R_{\text{int}} = 0.0260$
h	$-10 \rightarrow 11$,
k	$-19 \rightarrow 19$,
l	$-20 \rightarrow 19$
Final R indices [$F^2 > 2\sigma(F^2)$]	$R_1 = 0.0498$, $wR(F^2) = 0.1388$
Goodness of fit on $F^2(S)$	0.922
Parameters	202
Maximum shift	$(\Delta/\sigma)_{\text{max}} = 0.627$
Largest difference peak (e \AA^{-3})	$\Delta\rho_{\text{max}} = 1.053$
Largest hole (e \AA^{-3})	$\Delta\rho_{\text{min}} = -0.658$

The bond angles $\text{C9A-C8-Fe} = 77.8(3)^\circ$ and $\text{C9A-C8-Fe} = 71.7(3)^\circ$ are close to the 76.5° observed in the similarly coordinated bimetallic mixed-ligand complexes [23,24]. They are significantly smaller than the 119.2° reported for the corresponding angle in the neutral pentyl complex $[\text{Cp}^*(\text{CO})_2\text{Fe}(\text{C}_5\text{H}_{11})]$ [26]. The reduction indicates significant distortion in the ligand to allow for closer interaction between the metal and the ligand.

3. Conclusions

The NMR and crystallographic data for the monometallic carbocationic complex $[\text{Cp}(\text{CO})_2\text{Fe}\{\eta^2\text{-(CH}_2\text{CHCH}_2\text{CH}_3)\}] \text{PF}_6$ support the conclusion that the carbocationic ligand is coordinated to the metal in a η^2 -fashion forming a chiral metallacyclopropane structure. The coordination does not appear to be enantioface selective because both the *R* and *S* isomers are observed in the solid state in equal amounts. The structure observed in the solid state is retained in solution, suggesting strong bonds between the metal and the alkyl carbocation ligand.

4. Experimental

4.1. General

All manipulations were carried out under dry nitrogen using standard Schlenk line techniques. All solvents were dried and purified using appropriate methods before use [17]. Trifluoroacetic acid was used as obtained (Aldrich). Nuclear Magnetic Resonance spectra were recorded using Varian Inova 400 MHz and Varian Gemini 300 MHz spectrometers. The ^1H and ^{13}C NMR chemical shifts are reported in ppm downfield from tetramethylsilane (δ scale).

4.2. Synthesis of $[\text{Cp}(\text{CO})_2\text{Fe}\{\eta^2-(\text{CH}_2\text{CHCH}_2\text{CH}_3)\}]\text{PF}_6$

The compound $[\text{Cp}(\text{CO})_2\text{Fe}\{\eta^2-(\text{CH}_2\text{CHCH}_2\text{CH}_3)\}]\text{PF}_6$ was prepared by reacting $[\{\text{Cp}(\text{CO})_2\text{Fe}\}_2(\text{C}_4\text{H}_7)]\text{PF}_6$ with CF_3COOH in THF as previously described [17]. IR (cm^{-1} , CH_2Cl_2): ν_{CO} 2075, 2038; m.p. 124–125 °C dec.; ^1H NMR (acetone- d_6): $[\delta]$ 5.92s (Cp), 4.05d (1H, $J = 8.2$ Hz, *cis*- CH_2CH), 3.15d (1H, $J = 14.6$ Hz, *trans*- CH_2CH), 5.34m (1H, CH_2CH), 2.48m (1H, CHCH_2), 1.71m (1H, CHCH_2) 1.22m (3H, $J = 7.1$ Hz, CH_3); ^{13}C NMR (acetone- d_6): $[\delta]$ 211.5, 209.4 (CO), 90.9 (CH_2CH), 90.4 (Cp), 54.5 (CH_2CH), 30.3 (CH_2CH_3), 17.2 (CH_3). Anal. Calc. for $\text{C}_{11}\text{H}_{13}\text{F}_6\text{O}_2\text{PF}_6$: C, 34.95; H, 3.47. Found C, 34.82; H, 3.56%. These data agree with those reported for the same compound prepared by hydride abstraction [1].

4.3. Single crystal X-ray diffraction

X-ray quality crystals were obtained by slow diffusion of a twofold excess of hexane into a concentrated solution of $[\text{Cp}(\text{CO})_2\text{Fe}\{\eta^2-(\text{CH}_2\text{CHCH}_2\text{CH}_3)\}]\text{PF}_6$ in dichloromethane kept at 278 K over a period of six weeks. The X-ray diffraction intensity data were collected with an Oxford Excalibur 2 diffractometer (CrysAlis CCD 170) using Mo $\text{K}\alpha$ radiation ($\lambda = 0.71073$ Å) with a 2θ scan mode [27]. The structure was solved by direct methods using SHELXS97 [28] and refined using SHELXL97 [28]. The crystal, data collection and refinement information are summarized in Table 2. The hydrogen atoms were placed in calculated positions (the PART instruction was employed for the placing of the hydrogen atoms of the disordered C9 atom).

Acknowledgements

We acknowledge financial support from NRF, THRIP and UKZN (URF). E.O.C. thanks Kenyatta University, Kenya, for study leave to carry out this work.

Appendix A. Supplementary material

CCDC 662888 contains the supplementary crystallographic data for this paper. These data can be obtained free of charge from The Cambridge Crystallographic Data Centre via www.ccdc.cam.ac.uk/data_request/cif. Supplementary data associated with this article can be found, in the online version, at doi:10.1016/j.jorganchem.2007.10.014.

References

- [1] H.S. Clayton, J.R. Moss, M.E. Dry, *J. Organomet. Chem.* 688 (2003) 181.
- [2] M.L.H. Green, P.L.I. Nagy, *J. Am. Chem. Soc.* 84 (1962) 1310.
- [3] M.L.H. Green, P.L.I. Nagy, *Proc. Chem. Soc.* (1962) 74.
- [4] M.L.H. Green, P.L.I. Nagy, *J. Chem. Soc.* (1963) 189.
- [5] M.L.H. Green, P.L.I. Nagy, *J. Organomet. Chem.* 1 (1963) 58.
- [6] M. Rosenblum, *J. Organomet. Chem.* 300 (1986) 191, and references therein.
- [7] T.C.T. Chang, B.M. Foxman, M. Rosenblum, C. Stockman, *J. Am. Chem. Soc.* 103 (1981) 7361.
- [8] L.A. Watson, B. Franzman, J.C. Bollinger, K.G. Caulton, *New J. Chem.* 27 (2003) 1769.
- [9] T.-S. Peng, A.M. Arif, J.A. Gladysz, *Helv. Chim. Acta* 75 (1992) 442.
- [10] M. Sanau, T.-S. Peng, A.M. Arif, J.A. Gladysz, *J. Organomet. Chem.* 503 (1995) 235.
- [11] S.G. Bodnar, T.-S. Peng, A.M. Arif, J.A. Gladysz, *Organometallics* 9 (1990) 1191.
- [12] J.J. Kowalczyk, A.M. Arif, J.A. Gladysz, *Chem. Ber.* 124 (1991) 729.
- [13] J. Pu, T.-S. Peng, C.L. Mayne, A.M. Arif, J.A. Gladysz, *Organometallics* 12 (1993) 2686.
- [14] T.-S. Peng, A.M. Arif, J.A. Gladysz, *J. Chem. Soc., Dalton Trans.* (1995) 1857, and references therein.
- [15] O. Eisenstein, R. Hoffmann, *J. Am. Chem. Soc.* 102 (1980) 6148.
- [16] T.C.T. Chang, B.M. Foxman, M. Rosenblum, C. Stockman, *J. Am. Chem. Soc.* 103 (1981) 7362.
- [17] E.O. Changamu, H.B. Friedrich, *J. Organomet. Chem.* 692 (2007) 1138.
- [18] E.O. Changamu, H.B. Friedrich, M. Rademeyer, *J. Organomet. Chem.* 692 (2007) 2456.
- [19] W.P. Gierring, M. Rosenblum, J. Tancrede, *J. Am. Chem. Soc.* 94 (1972) 7170.
- [20] A. Cutler, D. Ehntholt, P. Lennon, K. Nicholas, D.F. Marten, M. Madhavarao, S. Raghu, A. Rosan, M. Rosenblum, *J. Am. Chem. Soc.* 97 (1975) 3149.
- [21] G. Paiaro, A. Panunzi, *J. Am. Chem. Soc.* 88 (1964) 5148.
- [22] E.O. Changamu, H.B. Friedrich, R.A.I. Howie, M. Rademeyer, *J. Organomet. Chem.* (2007), doi:10.1016/j.jorganchem.2007.07.030.
- [23] E.O. Changamu, H.B. Friedrich, M. Rademeyer, *Acta Crystallogr., Sect. E* 62 (2006) m442.
- [24] H.B. Friedrich, E.O. Changamu, M. Rademeyer, *Acta Crystallogr., Sect. E* 62 (2006) m405.
- [25] L. Pope, P. Sommerville, M. Laing, K.J. Hindson, J.R. Moss, *J. Organomet. Chem.* 112 (1976) 309.
- [26] R.O. Hill, C.F. Marais, J.R. Moss, K.J. Naidoo, *J. Organomet. Chem.* 587 (1999) 28.
- [27] Oxford Diffraction. CrysAlis CCD and CrysAlis RED. Versions 1.170. Oxford Diffraction Ltd., Abingdon, Oxfordshire, England, 2003.
- [28] G.M. Sheldrick, SHELXS97 and SHELXL97, University of Göttingen, Germany, 1997.